Targeting the Metastasis Suppressor, NDRG1, Using Novel Iron Chelators: Regulation of Stress Fiber-Mediated Tumor Cell Migration *via* Modulation of the ROCK1/pMLC2 Signaling Pathway

Jing Sun , Daohai Zhang , Ying Zheng, Qian Zhao, Minhua Zheng , Zaklina Kovacevic and Des R. Richardson

Department of General Surgery, Ruijin Hospital, Shanghai Jiao Tong University School of Medicine, Shanghai, P.R.China (J.S., M.Z.); Department of Pathology, University of Sydney, New South Wales, Australia (D.Z, Z.K., D.R.R.); Department of Pathophysiology, Key Laboratory of Cell Differentiation and Apoptosis of Chinese Ministry of Education, Shanghai Jiao Tong University School of Medicine, Shanghai, P.R.China (Y.Z., Q.Z.)

Running Title: NDRG1 and Stress Fiber-induced Cancer Migration

Author for correspondence: Dr. D. R. Richardson, Iron Metabolism and Chelation Program, Department of Pathology and Bosch Institute, University of Sydney, Sydney, New South Wales, 2006 Australia, Ph.: +61-2-9036-6548; +61-2-9036-6549; Fax: 61-2-9351-3429; Email: d.richardson@med.usyd.edu.au.

The number of text pages: 35

The number of tables: 0

The number of figures: 10 plus 6 Supplementary Figures

The number of references: 60

Word Count:

- *Abstract*: 250

- *Introduction*: 713

- *Discussion*: 961

Abbreviations:

DAPI, 4',6-diamidino-2-phenylindole; DFO, desferrioxamine; DMSO, dimethyl sulfoxide; Dp2mT, di-2-pyridylketone 2-methyl-3-thiosemicarbazone; Dp44mT, di-2-pyridylketone 4,4-dimethyl-3-thiosemicarbazone; DpC, di-2-pyridylketone 4-cyclohexyl-4-methyl-3-thiosemicarbazone; IOD, integrated optical density; MLC2, myosin light chain 2; NDRG1, N-myc downstream regulated gene-1; NIH, National Institutes of Health; pMLC2, phosphorylated myosin light chain 2; RhoA, ras homolog family member A; ROCK1, Rho-associated, coiled-coil containing protein kinase 1; shRNA, small hairpin RNA; siRNA, small interfering RNA; Y27632, (R)-(+)-trans-4-(1-Aminoethyl)-N-(4-pyridyl)cyclohexanecarboxamide dihydrochloride.

Abstract

The iron-regulated metastasis suppressor, N-myc downstream regulated gene-1 (NDRG1), is up-regulated by cellular iron depletion mediated by iron chelators and can inhibit cancer cell migration. However, the mechanism of how NDRG1 achieves this effect remains unclear. In this study, we implemented established and newly constructed NDRG1 over-expression and knockdown models using the DU145, HT29 and HCT116 cancer cell lines to investigate the molecular basis by which NDRG1 exerts its inhibitory effect on cell migration. Using these models, we demonstrated that NDRG1 over-expression inhibits cell migration by preventing actin-filament polymerization, stress fiber assembly and formation. In contrast, NDRG1 knockdown had the opposite effect. Moreover, we identified that NDRG1 inhibited an important regulatory pathway mediated by the Rho-associated, coiled-coil containing protein kinase 1 (ROCK1)/phosphorylated myosin light chain 2 (pMLC2) pathway that modulates stress fiber assembly. The phosphorylation of MLC2 is a key process in inducing stress fiber contraction and this was shown to be markedly decreased or increased by NDRG1 over-expression or knockdown, respectively. The mechanism involved in the inhibition of MLC2 phosphorylation by NDRG1 was mediated by a significant ($p<0.001$) decrease in ROCK1 expression that is a key kinase involved in MLC2 phosphorylation. Considering that NDRG1 is up-regulated after cellular iron depletion, novel thiosemicarbazone iron chelators (*e.g.*, di-2-pyridylketone 4,4-dimethyl-3-thiosemicarbazone) were demonstrated to inhibit ROCK1/pMLC2-modulated actin-filament polymerization, stress fiber assembly and formation *via* a mechanism involving NDRG1. These results highlight the role of the ROCK1/pMLC2 pathway in the NDRG1-mediated anti-metastatic signaling network and the therapeutic potential of iron chelators at inhibiting metastasis.

Introduction

Despite breakthroughs in therapy, prostate and colon tumors are major causes of cancer-related mortality (Siegel et al., 2012). Thus, new approaches to prostate and colorectal cancer treatment have focused on therapeutically targeting crucial molecules involved in disease progression (Fu et al., 2012; Tsujii, 2012). One newly identified molecular target, namely the metastasis suppressor, N-myc downstream regulated gene-1 (NDRG1), has been reported to inhibit prostate and colorectal cancer progression (Guan et al., 2000; Liu et al., 2011). In addition, *NDRG1* mRNA and protein levels were decreased in the primary tumor and metastases when compared to normal tissues (Kurdistani et al., 1998). Over-expression of NDRG1 in cancer cells not only induces differentiation (Fotovati et al., 2011), but also reduces invasion and metastasis (Chen et al., 2012). Several studies report a positive correlation between NDRG1 expression and patient survival, indicating NDRG1 may be a prognostic biomarker in prostate (Liu et al., 2011) and colorectal cancer (Guan et al., 2000). Although NDRG1 is largely considered to be a metastasis suppressor, several studies have also found this latter protein to be associated with increased metastasis and poor prognosis in certain neoplasms, such as hepatocellular carcinoma (Ellen et al., 2008). However, notably, the majority of studies have reported a tumor/metastasis suppressive role of NDRG1 (Ellen et al., 2008). The molecular pathways that NDRG1 affects are still unclear and require exploration, as this metastasis suppressor may be a useful therapeutic target.

Studies from our laboratory (Chen et al., 2012; Kovacevic et al., 2012; Le and Richardson, 2004; Lovejoy et al., 2011; Lovejoy et al., 2012; Whitnall et al., 2006; Yu et al., 2012) and others (Liu et al., 2012; Rao et al., 2009; Rao et al., 2011; Tian et al., 2010) have shown that novel iron-binding agents (*e.g.*, di-2-pyridylketone 4,4-dimethyl-3-thiosemicarbazone (Dp44mT) and di-2-pyridylketone 4-cyclohexyl-4-methyl-3-thiosemicarbazone (DpC); Fig. 1) possess marked and selective anti-tumor and anti-metastatic activity by up-regulating NDRG1. The mechanism involved occurs through the depletion of cellular iron *via* hypoxia-inducible factor 1α-dependent and -

independent pathways (Le and Richardson, 2004). Importantly, NDRG1 up-regulation by cellular iron-depletion inhibits the epithelial-mesenchymal transition that is crucial for metastasis (Chen et al., 2012). Apart from iron chelators, NDRG1 was also found to be up-regulated in response to other anti-cancer agents including hydroxyurea, cisplatin and doxorubicin (Delgado-Canedo et al., 2005; Mandal et al., 2004), further implicating its role in suppressing tumor progression.

Cell migration plays a crucial role in cancer cell metastasis. Considering the mechanism of cancer cell migration, actin participates in a range of events in cellular locomotion, including cell motility, cell polarity, cell junction function and chemotaxis (Dominguez and Holmes, 2011; Lai et al., 2012). Actin exists in the cytoplasm in two different forms, namely the actin monomer (G-actin) and actin filament (F-actin). When G-actin exchanges bound ADP for ATP, it is activated and polymerizes into F-actin bundles, also known as stress fibers (Dominguez and Holmes, 2011). When cancer cells make stable associations to a substrate, or when metastasis signaling pathways are triggered, stress fibers are rearranged and extend within the cell (Lai et al., 2012). Myosin interacts with F-actin to drive the movement of actin filaments past one another and the consequent fiber contraction causes alterations in cell shape and cellular migration (Tojkander et al., 2011).

It is reported that a key factor in stress fiber formation is the phosphorylation of myosin light chain 2 (MLC2) at Thr18/Ser19 (Katoh et al., 2011). Cells have a complicated signaling network modulating MLC2 phosphorylation, among which the Rho-associated, coiled-coil containing protein kinase 1 (ROCK1) pathway is one of the most crucial mechanisms in stimulating cross-linking of actin by myosin, leading to enhanced cancer cell contractility (Chaturvedi et al., 2011). Therefore, targeting the ROCK1/pMLC2 pathway to inhibit cancer cell migration may become a therapeutic strategy.

Considering the potent anti-metastatic effect of NDRG1 in various cancer cell-types and the role of

the ROCK1/pMLC2 pathway in activating stress fiber-mediated cell motility and migration, we examined whether the ROCK1/pMLC2 pathway played a critical role in NDRG1-mediated inhibition of cell migration. Our studies demonstrate a significant role of NDRG1 expression in inhibiting the ROCK1/pMLC2 pathway and provide novel insights into the mechanisms underlying the ability of NDRG1 to inhibit cell migration. Furthermore, this investigation illustrates that targeting NDRG1 using potent thiosemicarbazone chelators could be an important new approach to cancer treatment.

Materials and Methods

Cell Culture

The human prostate cancer cell line, DU145, and the human colon cancer cell lines, HT29 and HCT116, were from the American Type Culture Collection (ATCC, Manassas, VA) and were grown under established conditions (Chen et al., 2012).

Chelators and ROCK1 Inhibitor

Desferrioxamine (DFO; Fig. 1A) was purchased from Novartis (Basel, Swtizerland). The chelators, Dp44mT and DpC (Fig. 1B, C), and the negative control compound, Dp2mT (Fig. 1D) (Yuan et al., 2004), were synthesized and characterized using standard methods (Lovejoy et al., 2012; Yuan et al., 2004). The ROCK1 inhibitor, (+)-(R)-trans-4-(1-aminoethyl)-N-(4-pyridyl) cyclohexanecarboxamide dihydrochloride (Y27632) (Kuwahara et al., 1999), was from Abcam (Cambridge, UK).

Plasmid Construction/Transfection

NDRG1 over-expression and knockdown clones in DU145 and HT29 cell lines were established as described previously (Chen et al., 2012). The plasmids and shRNAs used for transfection of NDRG1 in HCT116 cells were pBABE-3×Flag-NDRG1 (from G. Chen, Shanghai Jiao Tong University, China) and pSIREN-shRNA (Clontech, Mountain View, CA), respectively. To over-express NDRG1, HCT116 cells were transfected using the pBABE-3×Flag-NDRG1 plasmid, while the pSIREN-shRNA plasmid containing NDRG1-specific shRNA (Chen et al., 2006; Stein et al., 2004; Zheng et al., 2009) was used to knockdown endogenous NDRG1 expression. All cDNAs were sequenced to ensure identity by BGI-Tech Ltd (Shanghai, China). Viral supernatants were produced in HEK293T cells co-transfected with the pBABE-3×Flag-control or pBABE-3×Flag-NDRG1 constructs and packaging vectors GAG-POL and VSV-G (Clontech). The HCT116 cells were transfected using the retrovirus system. Puromycin (2.5 μg/mL; Sigma-Aldrich) was used to

7

select stable single clones.

Transswell Migration and Wound-Healing Assay

The transwell migration assay was performed using the CytoSelect™ 24-Well Cell Migration Assay kit (Cell Biolabs, San Diego, CA) (Chen et al., 2012). For the wound-healing assay, the cell monolayer was scraped using a Gilson p200 pipette tip. After a 14-36 h incubation, the area covered by migrating cells was analyzed by Image J software (NIH, Bethesda, Maryland).

Gene Silencing by Small Interfering RNA (siRNA)

Knockdown of ROCK1 expression using ROCK1 siRNA was performed following the manufacturer's instructions. Briefly, at ~60-70% confluence, NDRG1-knockdown and sh-Control cells were transfected with ROCK1 Trilencer-27 siRNA duplexes (OriGene, Rockville, MD), or the scrambled control siRNA at 10 nM for 24 h, using Lipofectamine 2000® (Invitrogen).

Protein Extraction and Immunoblots

Preparation of cell lysates and immunoblot analysis were performed *via* established protocols (Kovacevic et al., 2008). Primary antibodies used include: NDRG1 (Cat. #: ab37897) from Abcam (Cambridge, UK); MLC2 (Cat. #: 3672) and pMLC2 (Cat. #: 3675) from Cell Signaling Technology (Beverly, MA); ROCK1 (Cat. #: WH0006093M1) and β-actin (Cat. #: A1978) from Sigma-Aldrich; and GAPDH (Cat. #: sc-32233) from Santa Cruz Biotechnology (Santa Cruz, CA). The secondary antibodies implemented include: horseradish peroxidase (HRP)-conjugated anti-goat (Cat.#: A5420), anti-rabbit (Cat. #: A6154) and anti-mouse (Cat. #: A4416) antibodies from Sigma.

Fractionation and Quantification Analysis of F-actin

F-actin extraction and fractionation were performed *via* established methods (Pan et al., 2011). Briefly, cells were harvested and homogenized using 27 G syringes in 500 μL of lysis and F-actin

stabilization buffer (50 mM piperazine-N,N'-bis (2-ethanesulfonic acid), 50 mM NaCl, 5 mM MgCl$_2$, 5 mM ethylene glycol tetraacetic acid, 5% glycerol, 0.1% Nonidet P-40, 0.1% Triton X-100, 0.1% Tween 20, and 0.1% β-mercaptoethanol, pH 6.9) at 37°C. The F-actin was then separated by ultra-centrifugation at 100,000×g for 60 min at 37°C. The pellets were resuspended in 500 μL ice-cold G-buffer (2 mM Tris-HCl pH 8.0, 0.2 mM CaCl$_2$, 0.2 mM ATP, and 0.5 mM dithiothreitol) and incubated on ice for 1 h (F-actin depolymerization). The dissociated F-actin was centrifuged at 14,000 × g for 10 min at 4°C. F-actin expression was then examined by immunoblots using a monoclonal anti-β-actin antibody (1:10000). GAPDH was utilized as the loading control.

Immunofluorescence

Immunofluorescence was performed as described (Chen et al., 2012). Fluorescence quantification was achieved by comparing the integrated optical density (IOD)/Area value of each protein of interest to the IOD/Area value of the nucleus (DAPI) in the same image. Images were captured using a Leica SPEII confocal microscope (63×; Leica, Heerbrugg, Switzerland). Raw images were analyzed using Metamorph software (Molecular Devices, Sunnyvale, CA). Co-localization analysis was performed using Imaris 7.3 (BITPLANE, Zurich, Switzerland).

Statistical Analysis

Data are expressed as mean ± standard deviation of ≥ 3 independent experiments and were statistically analyzed using Student's *t*-test. Results were considered significant when $p < 0.05$.

Results

NDRG1 Suppresses Cell Migration

The molecular effectors involved in the metastasis suppressor function of NDRG1 remain uncertain. To understand the role of NDRG1 in cancer cell migration which is a key characteristic of tumor metastasis, we utilized established and newly generated cell models that constitutively and stably over-express exogenous human NDRG1 in DU145 prostate cancer cells, as well as HT29 and HCT116 colorectal cancer cells (Fig. 2A). The DU145 prostate cancer cell line and HT29 colon cancer cell line are representative cell models of the two tumor-types where NDRG1 has been shown to play an important anti-metastatic role. These two cell models have been well characterized and the role of NDRG1 in the inhibition of cell migration and the epithelial-mesenchymal transition was clearly demonstrated in our previous studies (Chen et al., 2012). The third model, HCT116, is different from epithelial HT29 cells in terms of its cell phenotype and aggressiveness, and was introduced to assess if the response is consistent between cell lines.

In the 3 cell-types, exogenous expression of Flag-tagged NDRG1 was confirmed by immunoblots that demonstrated a band at ~45 kDa (Fig. 2A). In addition, the endogenously expressed NDRG1 was observed at ~43 and ~44 kDa, indicating a possible post-translational modification *e.g.*, phosphorylation (Kovacevic et al., 2011a; Murray et al., 2004). Considering this, it is notable that the densitometric analysis shown throughout this investigation represents the total of all NDRG1 bands. Clearly, the selected NDRG1 over-expressing clones generated from DU145, HT29 and HCT116 cells showed a significant ($p<0.001$) increase of NDRG1 expression compared to their respective empty vector-transfected control (Vector Control) cells (Fig. 2A).

To further understand the molecular effects of endogenous NDRG1, we also generated NDRG1-knockdown clones in these cancer cell lines. As indicated in Fig. 2A, compared to NDRG1 expression in control cells transfected with scrambled shRNA (sh-Control), the NDRG1-

knockdown clones showed a significant ($p<0.001$) ~5-20-fold reduction of total endogenous NDRG1 expression in DU145, HT29 and HCT116 cells.

Since cancer cell migration is one of the key factors deciding metastasis , and because NDRG1 is a metastasis suppressor (Ellen et al., 2008; Kitowska and Pawelczyk, 2010; Melotte et al., 2010), we investigated the effect of NDRG1 on cell migration using both the transwell (Fig. 2B) and wound healing assays (Supplemental Figure 1; see *Materials and Methods*). Using the transwell migration assay, we showed NDRG1 over-expression in DU145, HT29 and HCT116 cells resulted in a significant ($p<0.001$) 70%-90% reduction of migratory capacity compared to their respective Vector Control cells (Fig. 2B). On the other hand, NDRG1-knockdown in these cells led to a significant ($p<0.001$) 2.5-3.3-fold increase of migratory capacity (Fig. 2B). These observations further support the role of NDRG1 as a cell migration inhibitor (Chen et al., 2012; Hickok et al., 2011). Moreover, the inhibitory role of NDRG1 on cell migration was substantiated by studies using the wound-healing assay (Supplemental Figure 1). In fact, NDRG1 over-expression led to a significant ($p<0.001$) 32-44% decrease in cell migration into the wound area relative to the Vector Control cells in all three cell-types. Conversely, NDRG1 knockdown in these cell-types resulted in a significant ($p<0.001$) 1.5-2.2-fold increase of cells migrating into the wound relative to sh-Control cells (Supplemental Figure 1). Collectively, these results demonstrated that NDRG1 markedly inhibits migration of prostate and colorectal cancer cells.

NDRG1 Inhibits F-actin Polymerization and Stress Fiber Formation

The actin cytoskeleton is an important determinant of cell shape and migration (Suetsugu and Takenawa, 2003). Indeed, reorganization of the actin cytoskeleton plays a key role in driving migration and metastasis of cancer cells (Yamaguchi and Condeelis, 2007). Since NDRG1 acts to inhibit migration (Fig. 2B, Supplemental Figure 1), we further investigated its effects on actin filament polymerization and stress fiber formation. The total F-actin was fractionated from the

whole cell protein pool using well characterized procedures and detected using a β-actin antibody (Fig. 3A) (Kake et al., 1995; Kim et al., 2008; Pan et al., 2011). Hence, in these studies, GAPDH was utilized as a loading control. As shown in Fig. 3A, over-expression of NDRG1 in DU145, HT29 and HCT116 cells significantly ($p<0.001$-0.05) decreased the levels of F-actin, while knockdown of endogenous NDRG1 in these cells led to a significant ($p<0.001$) 2.7-3.8-fold increase of F-actin compared to their respective sh-Control cells. Therefore, for the first time, these results indicate an important inhibitory function of NDRG1 in F-actin synthesis.

We then examined whether NDRG1 could re-model the actin cytoskeleton and affect the distribution of F-actin in these cell models. In agreement with the results from immunoblot analysis (Fig. 3A), immunofluorescence staining of F-actin with rhodamine-phalloidin showed a significant ($p<0.01$-0.001) decrease or increase in staining intensity and stress fiber formation in the NDRG1-over-expressing or knockdown cells, respectively, relative to their controls (Fig. 3B-E).

In addition to the inhibitory effect of NDRG1 over-expression on F-actin synthesis, we also observed that NDRG1 over-expression or knockdown in these cell models affected cellular morphology and F-actin distribution (Fig. 3B-D). In DU145, HT29 and HCT116 Vector Control or sh-Control cells, F-actin was relatively evenly distributed between both the cytoplasm and at the circumference of the cell (so-called "cortical distribution"; see arrows in Fig. 3B-D). Notably, in DU145 cells, NDRG1 over-expression led to: *(i)* an increase in the size of the cells and *(ii)* an appearance of more epithelial-like phenotype (Fig. 3B). However, NDRG1 over-expression resulted in no marked alteration in the morphology of HCT116 or HT29 cells (Fig. 3C, D). Nevertheless, the over-expression of NDRG1 in all three cell lines led to a general decrease ($p<0.001$-0.01) in the intensity of F-actin staining (Fig. 3E).

The knockdown of NDRG1 in these 3 cell-types induced a significant remodeling of actin

filaments, leading to stress fiber formation (see white arrows), and a morphological change to a more aggressive phenotype (*e.g.*, fibroblast-like cells – especially for DU145) relative to sh-Control cells (Fig. 3B-D). These phenotypic alterations are in agreement with our previous studies demonstrating the effect of NDRG1 expression on maintaining an epithelial phenotype in cancer cells (Chen et al., 2012). In fact, the observed epithelial-like phenotype in the NDRG1-overexpressing DU145 cells was consistent with the enhanced expression and membrane localization of the epithelial cell markers, E-cadherin and β-catenin, as demonstrated in our previous study (Chen et al., 2012). Collectively, these morphological characteristics indicate that NDRG1 expression modulates cellular phenotype and stress fiber formation.

NDRG1 Inhibits the ROCK1/pMLC2 Pathway

Stress fibers form when a cancer cell makes stable connections to a substrate (Tojkander et al., 2012), or when metastasis signaling is triggered by activators (Singh et al., 2011; Tanner et al., 2010). Actin filaments are generally oriented toward the cell surface through their plus end and may overlap in more interior regions of the cell in anti-parallel arrays (Tojkander et al., 2012). During contraction of stress fibers, myosin mediates sliding of anti-parallel actin filaments and plays a key role in stress fiber stability and cell motility (Hotulainen and Lappalainen, 2006). Notably, phosphorylation of myosin light chain (MLC2) has been demonstrated to be a vital motor involved in motility (Chaturvedi et al., 2011; Katoh et al., 2011). Therefore, we investigated the expression and phosphorylation of MLC2 in our NDRG1 over-expression and knock-down models.

Immunoblots showed that the basal level of MLC2 was not significantly ($p>0.05$) altered when NDRG1 was over-expressed or knocked down in these cells (Fig. 4A-C). On the contrary, the relative MLC2 phosphorylation (*i.e.*, pMLC2/MLC2 ratio) was significantly ($p<0.001$-0.05) decreased in NDRG1 over-expressing DU145, HT29 and HCT116 cells (Fig. 4A-C). Moreover, sh-NDRG1 markedly ($p<0.001$) increased the pMLC2/MLC2 ratio by 2.4-3.7-fold over their

13

respective sh-Control cells in all 3 cell-types (Fig. 4A-C).

Given that NDRG1 modulates cytoskeleton re-organization (Fig. 3B-D) and MLC2 phosphorylation (Fig. 4), we then examined the mechanism behind these effects. We demonstrated that the level of one of the upstream regulators of MLC2 phosphorylation, ROCK1 (Wyckoff et al., 2006), was significantly ($p<0.001$) reduced by NDRG1 over-expression in our cell models (Fig. 4A-C). Additionally, ROCK1 expression was markedly ($p<0.001$) increased by 2.4-3.0-fold when NDRG1 was knocked down in all these cell lines (Fig. 4A-C). This indicated that NDRG1 can inhibit MLC2 phosphorylation through affecting ROCK1 expression.

Previous studies have established a close association of pMLC2 with stress fiber formation (Tojkander et al., 2012). In support of this, we also observed that pMLC2 was predominantly located in the cytoplasm and in proximity with the plasma membrane (Fig. 5A-C) and was co-localized with F-actin to form filament bundles (see white arrows, Supplemental Figure 2) when NDRG1 was knocked down. Consistent with the immunoblot results (Fig. 4A-C), the fluorescence intensity of pMLC2 was significantly ($p<0.001-0.01$) decreased by 36-48% in NDRG1 over-expressing DU145, HT29 and HCT116 cells compared to Vector Control cells (Fig. 5D). Conversely, NDRG1 knockdown led to a significant ($p<0.001-0.05$) increase of pMLC2 expression by 1.6-2.8-fold compared to sh-Control cells (Fig. 5D). Taken together, these data further support that the ROCK1/pMLC2 pathway plays an important role in NDRG1-mediated stress fiber formation and actin re-organization.

NDRG1 Regulates pMLC2 through Modulating ROCK1 Expression

The above studies showed that NDRG1 over-expression inhibited, while NDRG1-knockdown enhanced, the ROCK1/pMLC2 pathway (Figs. 4, 5). However, it is uncertain whether NDRG1 can directly regulate MLC2 phosphorylation or if it exerts its function through inhibiting its kinase,

14

ROCK1. To investigate this, further studies using NDRG1-knockdown cell models aimed to examine the effects of the well characterized ROCK1 inhibitor (Y27632; Fig. 6) or transient ROCK1 knockdown with ROCK1 siRNA (Fig. 7).

Since the ROCK1 inhibitor, Y27632, efficiently inhibits ROCK1 protein expression (Tan et al., 2012) and activity (Uehata et al., 1997), the NDRG1 knockdown cells and the sh-Control cells were incubated with Y27632 at the previously established dose of 0.25 μM (Tan et al., 2012; Uehata et al., 1997) for 48 h and ROCK1 expression and the pMLC2/MLC2 ratio were then examined (Fig. 6). We showed that Y27632 had no significant effect on NDRG1 expression in these cell models, thus excluding any non-specific effects of Y27632 on NDRG1 levels (Fig. 6A-C). However, after inhibition of ROCK1 activity using Y27632, the pMLC2/MLC2 ratio was also significantly ($p<0.001$) reduced in these cell models (Fig. 6A-C). Regardless of NDRG1 expression, suppression of MLC2 phosphorylation occurred in accordance with ROCK1 inhibition. Our results suggest that Y27632 was active in inhibiting ROCK1 protein expression and activity under the conditions used in our investigation, in good agreement with previous studies (Tan et al., 2012; Uehata et al., 1997). Furthermore, analysis of immunofluoresence intensity showed significant ($p<0.001$) inhibition of MLC2 phosphorylation and F-actin polymerization by Y27632 (Supplemental Figure 3).

To further substantiate the inhibition of pMLC2 by ROCK1, the 3 NDRG1-knockdown (sh-NDRG1) cell models and their respective sh-Control cells were treated with ROCK1-specific siRNA (si-ROCK1) to transiently reduce endogenous ROCK1 expression (Fig. 7). Transient treatment of these cells with ROCK1-specific siRNA significantly ($p<0.001$) reduced ROCK1 expression. Similarly to the results observed with cells treated with Y27632 (Fig. 6), incubation with si-ROCK1 did not significantly affect NDRG1 expression (Fig. 7A-C). Instead, while basal MLC2 expression was not significantly changed by decreased ROCK1 expression, the pMLC2/MLC2 ratio was significantly ($p<0.001$-0.01) attenuated compared to their relative control

cells treated with the si-Control. Notably, treatment with si-ROCK1 resulted in at least a 35% reduction of ROCK1 expression in all cell-types. This reduction led to at least a 55% decrease of phosphorylation of MLC. These results indicate that phosphorylation of MLC is sensitive to ROCK1 kinase. Taken together, the results above (Figs. 4-7) reveal that NDRG1 regulates MLC2 phosphorylation *via* modulating ROCK1 expression, and thus, its activity.

Novel Thiosemicarbazone Iron Chelators Modulate ROCK1/pMLC2

Our previous studies (Kovacevic et al., 2011a; Kovacevic et al., 2012; Kovacevic et al., 2008; Le and Richardson, 2004; Whitnall et al., 2006) and those of others (Liu et al., 2011; Liu et al., 2012) have demonstrated that novel thiosemicarbazone chelators (*e.g.*, Dp44mT and DpC) markedly up-regulate NDRG1 in tumor cells *in vitro* and *in vivo*. Furthermore, NDRG1 up-regulation in cancer cells is considered to be one of the mechanisms underlying the chelator-induced inhibition of growth and metastasis (Kovacevic et al., 2012; Le and Richardson, 2004; Liu et al., 2012; Whitnall et al., 2006). Because NDRG1 plays an important role in actin filament remodeling and stress fiber formation *via* the ROCK1/pMLC2 pathway, we then examined whether chelators have similar effects when these cell models were incubated with these agents. In these studies, di-2-pyridylketone 2-methyl-3-thiosemicarbazone (Dp2mT), was used as an appropriate negative control as it has a similar chemical structure to Dp44mT (Fig. 1), but has been designed not to bind iron or up-regulate NDRG1 (Le and Richardson, 2004; Yuan et al., 2004). The well-characterized "gold-standard" iron chelator, DFO (Chaston et al., 2003), was also implemented in this study as a positive control for cellular iron-depletion and NDRG1 up-regulation (Le and Richardson, 2004). Furthermore, NDRG1 over-expressing DU145, HT29 and HCT116 cells were included as positive controls (see lane labeled "NDRG1"; Fig. 8A-C).

The DU145, HT29 and HCT116 parental cells were incubated with DFO (100 μM), Dp44mT (10 μM) or DpC (10 μM) for 24 h and the levels of NDRG1, ROCK1, MLC2 and phosphorylated

MLC2 were examined by immunoblots. Notably, the higher concentration of DFO was used due to its poor membrane permeability relative to the lipophilic and highly membrane-permeable ligands, Dp44mT and DpC, while all agents were used at doses that were previously found to be effective at both mobilizing intracellular iron and inducing NDRG1 expression (Kovacevic et al., 2011a; Lovejoy et al., 2012; Richardson et al., 1994; Yuan et al., 2004). As shown in Fig. 8A-C, NDRG1 expression was markedly ($p<0.001$) increased after incubation with DFO, Dp44mT or DpC relative to cells treated with the Vehicle control and the negative control, Dp2mT (10 μM).

We also observed that ROCK1 expression was significantly ($p<0.001$) decreased in these chelator-treated cells relative to cells incubated with the Vehicle control or Dp2mT (Fig. 8A-C). Furthermore, while incubation with DFO, Dp44mT or DpC did not result in a significant change in basal MLC2 expression (Fig. 8A-C), the pMLC2/MLC2 ratio was significantly ($p<0.001$-0.01) reduced by these chelators compared to cells treated with Vehicle or Dp2mT (Fig. 8A-C). In line with the inhibition of ROCK1/pMLC2 observed in NDRG1 over-expressing cells (Fig. 4), the decrease in ROCK1/pMLC2 levels after incubation with DFO, Dp44mT or DpC was consistent with that mediated by NDRG1 up-regulation.

Novel Iron Chelators Modulate the ROCK1/pMLC2 Pathway via Up-Regulation of NDRG1

Since the ROCK1/pMLC2 pathway could be inhibited by NDRG1 over-expression (Fig. 4, 5) or chelator treatment (Figs. 8, Supplemental Figures 4-6), we next explored whether NDRG1 up-regulation is the essential mediator of the ability of chelators to inhibit the ROCK1/pMLC2 pathway (Fig. 9A-C). To this end, the NDRG1-knockdown clones (sh-NDRG1) and their respective sh-Control cells were incubated with chelators (*i.e.*, 100 μM DFO, 10 μM Dp44mT or 10 μM DpC), the negative control (10 μM Dp2mT), or the Vehicle (0.1% DMSO/medium) for 24 h. Non-transfected parental cells (labeled as "Control") were also used for each cell line as a comparison between the sh-Control and sh-NDRG1 transfections. As demonstrated in Fig. 9A-C, assessing the

DU145, HT29 and HCT116 sh-Control cells, chelator treatment (*i.e.*, DFO, Dp44mT or DpC) resulted in a pronounced ($p<0.001$) increase of NDRG1 expression by ~4-10-fold over cells incubated with the Vehicle or Dp2mT. In all 3 cell-types, upon the chelator-induced up-regulation of NDRG1, ROCK1 expression was significantly ($p<0.001$) decreased by up to 60-90% in these sh-Control cells, compared to cells incubated with the Vehicle or Dp2mT (Fig. 9A-C). Accordingly, the pMLC2/MLC2 ratio was also markedly reduced by 60-80% ($p<0.001$) when these cells were treated with chelators (Fig. 9A-C). Notably, when these cell models were treated with chelators (DFO, Dp44mT, or DpC), F-actin and pMLC2 were significantly ($p<0.001$) decreased as assessed by the quantitative analysis of immunofluoresence intensity, relative to cells treated with the Vehicle control or Dp2mT (Supplemental Figures 4-6). Collectively, the effect of chelators on ROCK1, F-actin and pMLC2 levels is consistent with the ability of these agents to up-regulate NDRG1.

When the NDRG1-knockdown (sh-NDRG1) DU145 and HCT116 cells were treated with DFO, Dp44mT or DpC, the increase in NDRG1 expression was less pronounced than that observed in the chelator-treated sh-Control cells (Fig. 9A, C). In fact, sh-NDRG1 HCT116 cells showed no increase in NDRG1 expression following treatment with the iron chelators when compared to the Vehicle and Dp2mT controls (Fig. 9C). However, in contrast, in HT29 cells the up-regulation of NDRG1 induced by Dp44mT and DpC was similar in the sh-NDRG1 and sh-Control cells, while DFO did not increase NDRG1 expression in sh-NDRG1 cells as much as in sh-Control cells (Fig. 9B). This observed variation in response to chelators after NDRG1-knockdown between cell-types may be related to differences in efficacy of shRNA at suppressing chelator-induced NDRG1 expression.

We also demonstrated that NDRG1 knockdown affected the chelator-inhibited ROCK1/pMLC2 pathway. Incubation of sh-Control DU145 cells with chelators (DFO, Dp44mT and DpC) decreased ROCK1 expression by 60-90% and the pMLC2/MLC2 ratio by ~75% relative to Vehicle- and Dp2mT-treated cells (Fig. 9A). In comparison, incubation of NDRG1-knockdown DU145 cells with

these chelators resulted in a 50-65% reduction of ROCK1 expression and a 40-45% decrease of the pMLC2/MLC2 ratio. These results suggest that the lower level of chelator-induced NDRG1 in the NDRG1-knockdown DU145 cells *versus* the sh-Control DU145 cells exerts significantly ($p<0.001$) less inhibitory effect on ROCK1 expression and the pMLC2/MLC2 ratio (Fig. 9A).

In NDRG1-knockdown and sh-Control HT29 cells where chelator treatments induced a similar level of NDRG1 expression, ROCK1 expression was reduced ($p<0.001$) by chelators by 55-80% in the sh-NDRG1 cells and by 65-70% in the sh-Control cells, whereas the pMLC2/MLC2 ratio was decreased ($p<0.001$) by 70-78% in the NDRG1 knockdown cells and by ~80% in the sh-Control cells (Fig. 9B). Hence, the similar effect of chelators on NDRG1 expression in the sh-Control and sh-NDRG1 HT29 cells resulted in similar responses in ROCK1 levels and the pMCL2/MLC2 ratio. In agreement with these studies, immunofluorescence experiments examining F-actin and pMLC levels in DU145 and HT29 cells demonstrated that the chelators significantly ($p<0.001$) reduced their levels in both sh-Control and sh-NDRG1 cells (Supplemental Figure 4B-C, Supplemental Figure 5B-C).

Contrary to the results obtained with HCT116 sh-Control cells where DFO, Dp44mT or DpC caused a pronounced decrease in ROCK1 expression and the pMLC2/MLC2 ratio (Fig. 9C), these chelators were unable to exert a similar effect on the ROCK1/pMLC2 pathway in the sh-NDRG1 HCT116 cells. This was probably due to the absence of chelator-induced NDRG1 up-regulation in sh-NDRG1 HCT116 clones (Fig. 9C). Hence, in this cell line, sh-NDRG1 showed the most pronounced effect at reducing NDRG1 expression amongst the 3 cell-types tested (Fig. 9A-C). These observations were further confirmed using immunofluorescence to examine F-actin and pMLC2 levels in HCT116 sh-Control and sh-NDRG1 cells, where the chelators markedly inhibited stress fiber formation in sh-Control cells, while having little effect in sh-NDRG1 cells (Supplemental Figure 6B-C). Failure of NDRG1 induction by chelators in the sh-NDRG1 HCT116

clones may result from the high level of internalized siRNA transcribed from the sh-NDRG1construct, and this could be a reason for the lack of inhibition of the ROCK1/pMLC2 pathway in this cell-type.

Critically, one could find it difficult to understand why sh-NDRG1 knockdown did not markedly inhibit induction of NDRG1 by chelators in DU145 cells and HT29 cells, while effectively preventing induction of NDRG1 expression in HCT116 (Fig. 9A-C). Considering the variation in response, it is notable that the chelators markedly induce NDRG1 expression, and the level of inhibition provided by the sh-NDRG1 construct is probably relatively lower in DU145 and HT29 cells (Fig. 9A, B). Hence, it failed to markedly antagonize chelator-induced NDRG1 expression. However, in sh-NDRG1 HCT116 cells, treatment with chelators was unable to induce NDRG1 expression, demonstrating effective inhibition by shNDRG1 (Fig. 9C). Clearly, a cell-type dependent factor is affecting the efficiency of sh-NDRG1 to reduce NDRG1 expression.

Collectively, suppression of endogenous NDRG1 expression by sh-NDRG1 in two cell lines interrupts the ability of chelators to induce NDRG1 expression relative to the sh-Control, leading to partial (DU145) or total (HCT116) loss of inhibition of ROCK1 expression and MLC2 phosphorylation. These data indicate that NDRG1 plays an important role in the effector function of novel chelators, such as DpC, on the ROCK1/pMLC2 pathway.

Discussion

The metastasis suppressor NDRG1 has been identified as an important molecular target for new therapeutics and can modulate multiple pathways during tumorigenesis and metastatic progression (Chen et al., 2012; Kovacevic et al., 2012; Kovacevic et al., 2011b; Liu et al., 2012). Herein, we identify a novel mechanism by which NDRG1 exerts its anti-metastatic effects in prostate and colorectal cancer cells. We demonstrate that NDRG1 can suppress cell migration, F-actin polymerization and stress fiber formation *via* inhibiting the ROCK1/pMLC2 pathway in prostate and colorectal cancer cells. Interestingly, while this effect was significant in all 3 cell models, the changes in F-actin, ROCK1 and pMCL2 in DU145 prostate cancer cells were less marked when compared to the HT29 and HCT116 cells, and this may be due to the genetic heterogeneity between these cancer cells.

The actin cytoskeleton has a fundamental role in tumor cell migration and movement (O'Neill, 2009). This is achieved by two mechanisms: **(1)** actin polymerization against the cellular membrane at the leading edge provides force (Pollard and Cooper, 2009) and **(2)** actin filaments together with myosin II filaments form stress fibers composed of contractile actomyosin structures which play key roles in cancer cell motility (Tojkander et al., 2012). While the mechanisms of actin filament networks and signaling pathways are well understood, the molecular mechanisms underlying the assembly of stress fibers remain to be elucidated (Michelot and Drubin, 2011). Considering this, we investigated the effects of NDRG1 on actin filaments in prostate and colorectal cancer cells. We showed that NDRG1 inhibits cell migration *via* its effects on regulating actin filament polymerization and stress fiber formation (Fig. 3, 5, Supplemental Figures 2-6).

It has been well-established that there are cellular signaling networks which regulate stress fiber assembly and contraction (Tojkander et al., 2012). Among these pathways, the small GTPase RhoA, as well as its effector, ROCK, directly promote stress fiber assembly (Leung et al., 1996). In

addition, stress fiber contractility is regulated by MLC2 phosphorylation (Somlyo and Somlyo, 2000). Furthermore, MLC2 phosphorylation-mediated contractility of stress fibers is also Rho-dependent (Katoh et al., 2001). The RhoA/ROCK cascade results in actomyosin activity through direct phosphorylation of MLC2, generating contractile responses (Amano et al., 1996). Rho-kinases, such as ROCK, have also been demonstrated to regulate MLC2 phosphorylation in the invading margin of tumor cells, indicating its important role in modulating cancer cell migration, invasion and metastasis (Wyckoff et al., 2006) (Fig. 10). In our investigation, we showed that Rho-kinase ROCK1 promotes MLC2 phosphorylation and that NDRG1 inhibits MLC2 phosphorylation through down-regulating ROCK1. Thus, our studies establish a novel function of NDRG1 in modulating the ROCK1/pMLC2 pathway (Fig. 10).

Considering that NDRG1 plays an important role in regulating actin filament re-organization and stress fiber formation through modulating the ROCK1/pMLC2 pathway, we then examined the novel thiosemicarbazone iron chelators, Dp44mT and DpC, and the clinically used iron chelator, DFO, which can up-regulate NDRG1 *via* both HIF1α-dependent and -independent mechanisms and have selective anti-cancer activity (Chen et al., 2012; Kovacevic et al., 2011a; Kovacevic et al., 2012; Le and Richardson, 2004; Lovejoy et al., 2012; Whitnall et al., 2006; Yuan et al., 2004). Upon chelator-mediated up-regulation of NDRG1, the ROCK1/pMLC2 pathway was markedly suppressed and stress fiber formation was significantly reduced. This indicates the potential general effect of iron chelators on actin filament re-organization and stress fiber formation in cancer cells.

In agreement with our study, it has been reported in rat pulmonary artery endothelial cells that F-actin polymerization and cellular remodeling can be induced by iron supplementation (Gorbunov et al., 2012). Furthermore, iron-induced re-arrangements of the cytoskeleton can be partially eliminated in the presence of the iron chelator, *N,N*'-bis-(2-hydroxybenzyl)-ethylenediamine-*N,N*'-diacetic acid (Gorbunov et al., 2012). However, these latter investigations did not dissect the

molecular mechanisms involved, nor did they elucidate any role for NDRG1 in the processes observed. In contrast, our mechanistic studies showed that iron chelators inhibit cytoskeleton remodeling and cell migration through targeting the NDRG1/ROCK1/pMLC2 pathway.

It is notable that of the thiosemicarbazones utilized in the current study, DpC shows marked and selective anti-tumor activity both *in vitro* and *in vivo* (Kovacevic et al., 2011a; Kovacevic et al., 2012; Lovejoy et al., 2012). Indeed, this ligand has recently been shown to be active *via* both the oral and intravenous routes *in vivo* using pancreatic and lung cancer xenograft models (Kovacevic et al., 2011a; Kovacevic et al., 2012; Lovejoy et al., 2012). An important pharmacological advantage of DpC relative to its predecessor, Dp44mT (Whitnall et al., 2006), is that the agent does not induce cardiotoxicity even when administered at substantially higher doses (Lovejoy et al., 2012). Furthermore, unlike Dp44mT which results in toxicity when administered by the oral route (Yu et al., 2012), DpC demonstrates marked anti-tumor efficacy and tolerability when given *via* gavage (Lovejoy et al., 2012). Apart from these important pharmacological properties, the efficacy of DpC in up-regulating NDRG1 in addition to its effects on other key molecular targets *e.g.*, cyclin D1 (Kovacevic et al., 2011a), indicate the marked potential of this chelator as a novel anti-cancer agent.

In summary, this study demonstrates that NDRG1 is able to inhibit actin filament polymerization, stress fiber assembly and cell migration through modulating the ROCK1/pMLC2 pathway (see schematic: Fig. 10). Furthermore, novel iron chelators inhibit the ROCK1/pMLC2 pathway *via* up-regulation of NDRG1. Although the effect of chelators is, in part, to induce NDRG1 expression that results in inhibition of stress fiber formation, the mechanism may not be as straightforward as depicted in Fig 10. However, this schematic provides an instructive summary of the current studies and is an appropriate working model for further experimentation. In fact, our current results elucidate the underlying mechanism of the anti-metastatic effects of NDRG1 mediated through

inhibition of cellular migration and further identify novel iron chelators that target NDRG1 as a

promising therapy.

Authorship Contributions

Participated in research design: Sun, Zhang, Kovacevic, and Richardson.

Conducted experiments: Sun.

Contributed new reagents or analytic tools: Sun, Richardson.

Performed data analysis: Sun, Zhang, Kovacevic, and Richardson.

Wrote or contributed to the writing of the manuscript: Sun, Zhang, Y. Zheng, M. Zheng, Zhao,

Kovacevic, and Richardson.

References

Amano M, Ito M, Kimura K, Fukata Y, Chihara K, Nakano T, Matsuura Y and Kaibuchi K (1996) Phosphorylation and activation of myosin by Rho-associated kinase (Rho-kinase). *J Biol Chem* **271**(34):20246-20249.

Chaston TB, Lovejoy DB, Watts RN and Richardson DR (2003) Examination of the antiproliferative activity of iron chelators: multiple cellular targets and the different mechanism of action of triapine compared with desferrioxamine and the potent pyridoxal isonicotinoyl hydrazone analogue 311. *Clin Cancer Res* **9**(1):402-414.

Chaturvedi LS, Marsh HM and Basson MD (2011) Role of RhoA and its effectors ROCK and mDia1 in the modulation of deformation-induced FAK, ERK, p38, and MLC motogenic signals in human Caco-2 intestinal epithelial cells. *Am J Physiol Cell Physiol* **301**(5):C1224-1238.

Chen B, Nelson DM and Sadovsky Y (2006) N-myc down-regulated gene 1 modulates the response of term human trophoblasts to hypoxic injury. *J Biol Chem* **281**(5):2764-2772.

Chen Z, Zhang D, Yue F, Zheng M, Kovacevic Z and Richardson DR (2012) The iron chelators Dp44mT and DFO inhibit TGF-beta-induced epithelial-mesenchymal transition via up-regulation of N-myc downstream regulated gene 1 (NDRG1). *J Biol Chem* **287**(21):17016-17028.

Delgado-Canedo A, Chies JA and Nardi NB (2005) Induction of fetal haemoglobin expression in erythroid cells--a model based on iron availability signalling. *Med Hypotheses* **65**(5):932-936.

Dominguez R and Holmes KC (2011) Actin structure and function. *Annu Rev Biophys* **40**:169-186.

Ellen TP, Ke Q, Zhang P and Costa M (2008) NDRG1, a growth and cancer related gene: regulation of gene expression and function in normal and disease states. *Carcinogenesis* **29**(1):2-8.

Fotovati A, Abu-Ali S, Kage M, Shirouzu K, Yamana H and Kuwano M (2011) N-myc downstream-regulated gene 1 (NDRG1) a differentiation marker of human breast cancer. *Pathol Oncol Res* **17**(3):525-533.

Fu W, Madan E, Yee M and Zhang H (2012) Progress of molecular targeted therapies for prostate cancers. *Biochim Biophys Acta* **1825**(2):140-152.

Gorbunov NV, Atkins JL, Gurusamy N and Pitt BR (2012) Iron-induced remodeling in cultured rat pulmonary artery endothelial cells. *Biometals* **25**(1):203-217.

Guan RJ, Ford HL, Fu Y, Li Y, Shaw LM and Pardee AB (2000) Drg-1 as a differentiation-related, putative metastatic suppressor gene in human colon cancer. *Cancer Res* **60**(3):749-755.

Hickok JR, Sahni S, Mikhed Y, Bonini MG and Thomas DD (2011) Nitric oxide suppresses tumor cell migration through N-Myc downstream-regulated gene-1 (NDRG1) expression: role of chelatable iron. *J Biol Chem* **286**(48):41413-41424.

Hotulainen P and Lappalainen P (2006) Stress fibers are generated by two distinct actin assembly mechanisms in motile cells. *J Cell Biol* **173**(3):383-394.

Kake T, Kimura S, Takahashi K and Maruyama K (1995) Calponin induces actin polymerization at low ionic strength and inhibits depolymerization of actin filaments. *Biochem J* **312 (Pt 2)**:587-592.

Katoh K, Kano Y, Amano M, Onishi H, Kaibuchi K and Fujiwara K (2001) Rho-kinase--mediated contraction of isolated stress fibers. *J Cell Biol* **153**(3):569-584.

Katoh K, Kano Y and Noda Y (2011) Rho-associated kinase-dependent contraction of stress fibres and the organization of focal adhesions. *J R Soc Interface* **8**(56):305-311.

Kim HR, Gallant C, Leavis PC, Gunst SJ and Morgan KG (2008) Cytoskeletal remodeling in differentiated vascular smooth muscle is actin isoform dependent and stimulus dependent. *Am J Physiol Cell Physiol* **295**(3):C768-778.

Kitowska A and Pawelczyk T (2010) N-myc downstream regulated 1 gene and its place in the cellular machinery. *Acta Biochim Pol* **57**(1):15-21.

Kovacevic Z, Chikhani S, Lovejoy DB and Richardson DR (2011a) Novel thiosemicarbazone iron chelators induce up-regulation and phosphorylation of the metastasis suppressor N-myc down-stream regulated gene 1: a new strategy for the treatment of pancreatic cancer. *Mol Pharmacol* **80**(4):598-609.

Kovacevic Z, Chikhani S, Lui GY, Sivagurunathan S and Richardson DR (2012) The iron-regulated metastasis suppressor NDRG1 targets NEDD4L, PTEN, and SMAD4 and inhibits the PI3K and Ras signaling pathways. *Antioxid Redox Signal*(In Press; PMID: 22462691).

Kovacevic Z, Fu D and Richardson DR (2008) The iron-regulated metastasis suppressor, Ndrg-1: identification of novel molecular targets. *Biochim Biophys Acta* **1783**(10):1981-1992.

Kovacevic Z, Sivagurunathan S, Mangs H, Chikhani S, Zhang D and Richardson DR (2011b) The metastasis suppressor, N-myc downstream regulated gene 1 (NDRG1), upregulates p21 via p53-independent mechanisms. *Carcinogenesis* **32**(5):732-740.

Kurdistani SK, Arizti P, Reimer CL, Sugrue MM, Aaronson SA and Lee SW (1998) Inhibition of tumor cell growth by RTP/rit42 and its responsiveness to p53 and DNA damage. *Cancer Res* **58**(19):4439-4444.

Kuwahara K, Saito Y, Nakagawa O, Kishimoto I, Harada M, Ogawa E, Miyamoto Y, Hamanaka I, Kajiyama N, Takahashi N, Izumi T, Kawakami R, Tamura N, Ogawa Y and Nakao K (1999) The effects of the selective ROCK inhibitor, Y27632, on ET-1-induced hypertrophic response in neonatal rat cardiac myocytes--possible involvement of Rho/ROCK pathway in cardiac muscle cell hypertrophy. *FEBS Lett* **452**(3):314-318.

Lai Y, Liu XH, Zeng Y, Zhang Y, Shen Y and Liu Y (2012) Interleukin-8 induces the endothelial cell migration through the Rac 1/RhoA-p38MAPK pathway. *Eur Rev Med Pharmacol Sci* **16**(5):630-638.

Le NT and Richardson DR (2004) Iron chelators with high antiproliferative activity up-regulate the expression of a growth inhibitory and metastasis suppressor gene: a link between iron metabolism and proliferation. *Blood* **104**(9):2967-2975.

Leung T, Chen XQ, Manser E and Lim L (1996) The p160 RhoA-binding kinase ROK alpha is a member of a kinase family and is involved in the reorganization of the cytoskeleton. *Mol Cell Biol* **16**(10):5313-5327.

Liu W, Iiizumi-Gairani M, Okuda H, Kobayashi A, Watabe M, Pai SK, Pandey PR, Xing F, Fukuda K, Modur V, Hirota S, Suzuki K, Chiba T, Endo M, Sugai T and Watabe K (2011) KAI1 gene is engaged in NDRG1 gene-mediated metastasis suppression through the ATF3-NFkappaB complex in human prostate cancer. *J Biol Chem* **286**(21):18949-18959.

Liu W, Xing F, Iiizumi-Gairani M, Okuda H, Watabe M, Pai SK, Pandey PR, Hirota S, Kobayashi A, Mo YY, Fukuda K, Li Y and Watabe K (2012) N-myc downstream regulated gene 1 modulates Wnt-beta-catenin signalling and pleiotropically suppresses metastasis. *EMBO Mol Med* **4**(2):93-108.

Lovejoy DB, Jansson PJ, Brunk UT, Wong J, Ponka P and Richardson DR (2011) Antitumor activity of metal-chelating compound Dp44mT is mediated by formation of a redox-active copper complex that accumulates in lysosomes. *Cancer Res* **71**(17):5871-5880.

Lovejoy DB, Sharp DM, Seebacher N, Obeidy P, Prichard T, Stefani C, Basha MT, Sharpe PC, Jansson PJ, Kalinowski DS, Bernhardt PV and Richardson DR (2012) Novel second-generation di-2-pyridylketone thiosemicarbazones show synergism with standard chemotherapeutics and demonstrate potent activity against lung cancer xenografts after oral and Intravenous administration in Vivo. *J Med Chem* **55**(16):7230-7244.

Mandal R, Kalke R and Li XF (2004) Interaction of oxaliplatin, cisplatin, and carboplatin with hemoglobin and the resulting release of a heme group. *Chem Res Toxicol* **17**(10):1391-1397.

Melotte V, Qu X, Ongenaert M, van Criekinge W, de Bruine AP, Baldwin HS and van Engeland M (2010) The N-myc downstream regulated gene (NDRG) family: diverse functions, multiple applications. *FASEB J* **24**(11):4153-4166.

Michelot A and Drubin DG (2011) Building distinct actin filament networks in a common cytoplasm. *Curr Biol* **21**(14):R560-569.

Murray JT, Campbell DG, Morrice N, Auld GC, Shpiro N, Marquez R, Peggie M, Bain J, Bloomberg GB, Grahammer F, Lang F, Wulff P, Kuhl D and Cohen P (2004) Exploitation of KESTREL to identify NDRG family members as physiological substrates for SGK1 and GSK3. *Biochem J* **384**(Pt 3):477-488.

O'Neill GM (2009) The coordination between actin filaments and adhesion in mesenchymal migration. *Cell Adh Migr* **3**(4):355-357.

Pan SH, Chao YC, Hung PF, Chen HY, Yang SC, Chang YL, Wu CT, Chang CC, Wang WL, Chan WK, Wu YY, Che TF, Wang LK, Lin CY, Lee YC, Kuo ML, Lee CH, Chen JJ, Hong TM and Yang PC (2011) The ability of LCRMP-1 to promote cancer invasion by enhancing filopodia formation is antagonized by CRMP-1. *J Clin Invest* **121**(8):3189-3205.

Pollard TD and Cooper JA (2009) Actin, a central player in cell shape and movement. *Science* **326**(5957):1208-1212.

Rao VA, Klein SR, Agama KK, Toyoda E, Adachi N, Pommier Y and Shacter EB (2009) The iron chelator Dp44mT causes DNA damage and selective inhibition of topoisomerase IIalpha in breast cancer cells. *Cancer Res* **69**(3):948-957.

Rao VA, Zhang J, Klein SR, Espandiari P, Knapton A, Dickey JS, Herman E and Shacter EB (2011) The iron chelator Dp44mT inhibits the proliferation of cancer cells but fails to protect from doxorubicin-induced cardiotoxicity in spontaneously hypertensive rats. *Cancer Chemother Pharmacol* **68**(5):1125-1134.

Richardson D, Ponka P and Baker E (1994) The effect of the iron(III) chelator, desferrioxamine, on iron and transferrin uptake by the human malignant melanoma cell. *Cancer Res* **54**(3):685-689.

Siegel R, Naishadham D and Jemal A (2012) Cancer statistics, 2012. *CA Cancer J Clin* **62**(1):10-29.

Singh S, Wu S, Varney M, Singh AP and Singh RK (2011) CXCR1 and CXCR2 silencing modulates CXCL8-dependent endothelial cell proliferation, migration and capillary-like structure formation. *Microvasc Res* **82**(3):318-325.

Somlyo AP and Somlyo AV (2000) Signal transduction by G-proteins, rho-kinase and protein phosphatase to smooth muscle and non-muscle myosin II. *J Physiol* **522 Pt 2**:177-185.

Stein S, Thomas EK, Herzog B, Westfall MD, Rocheleau JV, Jackson RS, 2nd, Wang M and Liang P (2004) NDRG1 is necessary for p53-dependent apoptosis. *J Biol Chem* **279**(47):48930-48940.

Suetsugu S and Takenawa T (2003) Regulation of cortical actin networks in cell migration. *Int Rev Cytol* **229**:245-286.

Tan H, Zhong Y, Shen X, Cheng Y, Jiao Q and Deng L (2012) Erythropoietin promotes axonal regeneration after optic nerve crush in vivo by inhibition of RhoA/ROCK signaling pathway. *Neuropharmacology* **63**(6):1182-1190.

Tanner K, Boudreau A, Bissell MJ and Kumar S (2010) Dissecting regional variations in stress fiber mechanics in living cells with laser nanosurgery. *Biophys J* **99**(9):2775-2783.

Tian J, Peehl DM, Zheng W and Knox SJ (2010) Anti-tumor and radiosensitization activities of the iron chelator HDp44mT are mediated by effects on intracellular redox status. *Cancer Lett* **298**(2):231-237.

Tojkander S, Gateva G and Lappalainen P (2012) Actin stress fibers--assembly, dynamics and biological roles. *J Cell Sci* **125**(Pt 8):1855-1864.

Tojkander S, Gateva G, Schevzov G, Hotulainen P, Naumanen P, Martin C, Gunning PW and Lappalainen P (2011) A molecular pathway for myosin II recruitment to stress fibers. *Curr Biol* **21**(7):539-550.

Tsujii M (2012) Search for novel target molecules for the effective treatment or prevention of colorectal cancer. *Digestion* **85**(2):99-102.

Uehata M, Ishizaki T, Satoh H, Ono T, Kawahara T, Morishita T, Tamakawa H, Yamagami K, Inui J, Maekawa M and Narumiya S (1997) Calcium sensitization of smooth muscle mediated by a Rho-associated protein kinase in hypertension. *Nature* **389**(6654):990-994.

Whitnall M, Howard J, Ponka P and Richardson DR (2006) A class of iron chelators with a wide

spectrum of potent antitumor activity that overcomes resistance to chemotherapeutics. *Proc Natl Acad Sci U S A* **103**(40):14901-14906.

Wyckoff JB, Pinner SE, Gschmeissner S, Condeelis JS and Sahai E (2006) ROCK- and myosin-dependent matrix deformation enables protease-independent tumor-cell invasion in vivo. *Curr Biol* **16**(15):1515-1523.

Yamaguchi H and Condeelis J (2007) Regulation of the actin cytoskeleton in cancer cell migration and invasion. *Biochim Biophys Acta* **1773**(5):642-652.

Yu Y, Suryo Rahmanto Y and Richardson DR (2012) Bp44mT: an orally active iron chelator of the thiosemicarbazone class with potent anti-tumour efficacy. *Br J Pharmacol* **165**(1):148-166.

Yuan J, Lovejoy DB and Richardson DR (2004) Novel di-2-pyridyl-derived iron chelators with marked and selective antitumor activity: in vitro and in vivo assessment. *Blood* **104**(5):1450-1458.

Zheng Y, Wang LS, Xia L, Han YH, Liao SH, Wang XL, Cheng JK and Chen GQ (2009) NDRG1 is down-regulated in the early apoptotic event induced by camptothecin analogs: the potential role in proteolytic activation of PKC delta and apoptosis. *Proteomics* **9**(8):2064-2075.

Footnotes

J.S. and D.Z. contribute equally as first authors. M.Z., Z.K. and D.R.R. contribute equally as co-corresponding authors.

Reprint requests to be sent to Prof. Des R. Richardson (Room 555, Blackburn Building D06, University of Sydney, NSW 2006, Australia). Email: d.richardson@med.usyd.edu.au

The authors declare no conflict of interest.

Figure Legends

Figure 1. Line drawings of the chemical structures of: (A) DFO, (B) Dp44mT, (C) DpC and (D) Dp2mT.

Figure 2. NDRG1 suppresses cell motility and migration of prostate and colorectal cancer cells. The DU145, HT29 and HCT116 cancer cell lines were stably transfected with NDRG1 over-expression and sh-NDRG1 knockdown vectors. **(A)** Whole cell lysates were extracted and immunoblotting was performed to assess NDRG1 over-expression and knockdown compared to their relative control cells (Vector Control and sh-Control, respectively). Densitometric analysis is expressed relative to the loading control, β-actin. **(B)** DU145, HT29 and HCT116 NDRG1-over-expressing and NDRG1-knockdown cells as well as their relative control cells were seeded at 100,000 cells/well and incubated for 24 h/37°C. Migratory cells on the bottom of the polycarbonate membrane were stained with crystal violet and images were then captured. Migration was quantified by colorimetric determination at 560 nm. Scale bars: 200 μm. Results are typical of 3-5 experiments and the histogram values are mean ± SD (3-5 experiments). *** $p<0.001$, relative to respective control cells.

Figure 3. NDRG1 expression inhibits F-actin polymerization and stress fiber formation in prostate and colorectal cancer cells. **(A)** F-actin was fractionated and quantified by immunoblot in NDRG1-over-expressing and NDRG1-knockdown DU145, HT29 and HCT116 relative to their control cells (Vector Control and sh-Control, respectively) using a well-established technique (see *Materials and Methods*). Densitometric analyses are expressed relative to the loading control, GAPDH. Data are typical of 3-5 experiments and the histogram values are mean ± SD (3-5 experiments). * $p<0.05$, ** $p<0.01$, *** $p<0.001$, relative to respective control cells. **(B-D)** Merged immunofluorescence images demonstrating F-actin (red) stained with rhodamine phalloidin and cell nucleus (blue) stained with DAPI in NDRG1-over-expressing and NDRG1-knockdown DU145,

HT29 and HCT116 cells relative to the Vector Control and sh-Control cells, respectively. White arrows indicate stress fibers. Scale bar: 25 μm. **(E)** Fluorescence quantification was performed by comparing the integrated optical density (IOD)/Area value of F-actin to the IOD/Area value of the nucleus (DAPI) in the same image. Results are typical of 3-5 images from different visual fields and the histogram values are mean ± SD (3-5 images). ** $p<0.01$, *** $p<0.001$, relative to the respective control cells.

Figure 4. NDRG1 mediates the ROCK1/pMLC2 pathway in prostate and colorectal cancer cells. NDRG1-over-expression can reduce ROCK1 expression and the pMLC2/MLC2 ratio, while NDRG1-knockdown can enhance ROCK1 expression and the pMLC2/MLC2 ratio in: **(A)** DU145 cells, **(B)** HT29 cells and **(C)** HCT116 cells compared to their relative control cells (*i.e.*, Vector Control and sh-Control, respectively). Densitometric analyses for NDRG1 and ROCK1 in **(A-C)** are expressed relative to the loading control, β-actin, while that for MLC2 phosphorylation in **(A-C)** is expressed as the pMLC2/MLC2 ratio. Results are typical of 3-5 experiments and the values in histograms in **(A-C)** represent mean ± SD (3-5 experiments). * $p<0.05$, *** $p<0.001$, relative to the respective control cells.
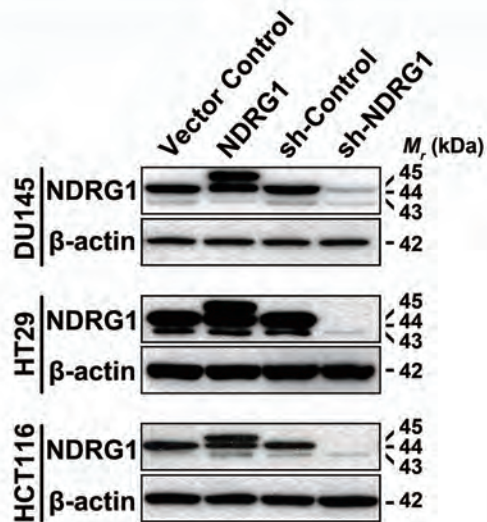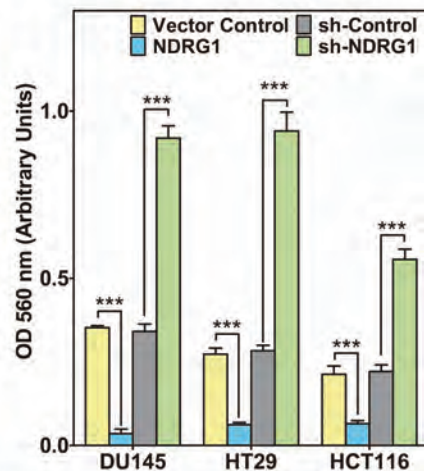
Figure 5. NDRG1 modulates cytoskeleton re-organization and MLC2 phosphorylation. **(A-C)** Merged immunofluorescence images demonstrate F-actin (red) stained with rhodamine phalloidin, pMLC2 (green) stained with Alexa Fluor® 488 and the cell nucleus (blue) stained with DAPI in NDRG1-over-expressing and NDRG1-knockdown DU145, HT29 and HCT116 cells respectively, compared to their relative control cells (*i.e.*, Vector Control and sh-Control, respectively). There was marked co-localization between F-actin and pMLC2 in all three cell-types after NDRG1 knockdown. Scale bars: 25 μm. **(D)** Fluorescence quantification was performed by comparing the integrated optical density (IOD)/Area value of pMLC2 to the IOD/Area value of nucleus (DAPI) in the same image. Results are typical of 3-5 images from different visual fields and the histogram

values are mean ± SD (3-5 images). * $p<0.05$, ** $p<0.01$, *** $p<0.001$, relative to the respective control cells.

Figure 6. Y27632 inhibits the ROCK1/pMLC2 pathway *via* an NDRG1-independent mechanism. (A-C) The sh-Control cells and sh-NDRG1 knockdown DU145, HT29 and HCT116 cells were treated with or without Y27632 (0.25 μM) for 48 h and the levels of NDRG1, ROCK1, pMLC2 and MLC2 were examined by immunoblot. **(A-C)** Densitometric analyses for NDRG1 and ROCK1 are expressed relative to the loading control, β-actin, while that for MLC2 phosphorylation is expressed as the pMLC2/MLC2 ratio. Results are typical of 3-5 experiments and the histograms in **(A-C)** represent mean ± SD (3-5 experiments). *** $p<0.001$, relative to the respective control cells incubated with medium only.

Figure 7. ROCK1-specific siRNA inhibits the ROCK1/pMLC2 pathway *via* an NDRG1-independent mechanism. (A-C) The sh-NDRG1 knockdown and sh-Control DU145, HT29 and HCT116 cells were incubated with scrambled control siRNA (si-Control) or ROCK1-specific siRNA (si-ROCK1) and the levels of NDRG1, ROCK1, pMLC2 and MLC2 were examined by immunoblot. Densitometric analysis for NDRG1 and ROCK1 are expressed relative to the loading control, β-actin, while that for MLC2 phosphorylation is expressed as the pMLC2/MLC2 ratio. Results are typical of 3-5 experiments and the histograms in **(A-C)** represent mean ± SD (3-5 experiments). ** $p<0.01$, *** $p<0.001$, relative to the respective si-Control cells.

Figure 8. Iron chelators modulate ROCK1/pMLC2 levels in prostate and colorectal cancer cells. (A) DU145, **(B)** HT29 and **(C)** HCT116 parental cells were treated with the chelators, DFO (100 μM), Dp44mT (10 μM), or DpC (10 μM) for 24 h and the levels of NDRG1, ROCK1, pMLC2 and MLC2 were examined by immunoblot. Vehicle (0.1% DMSO/medium) or Dp2mT (10 μM) were used as negative controls. Cells transfected with an NDRG1-expression vector were used as a
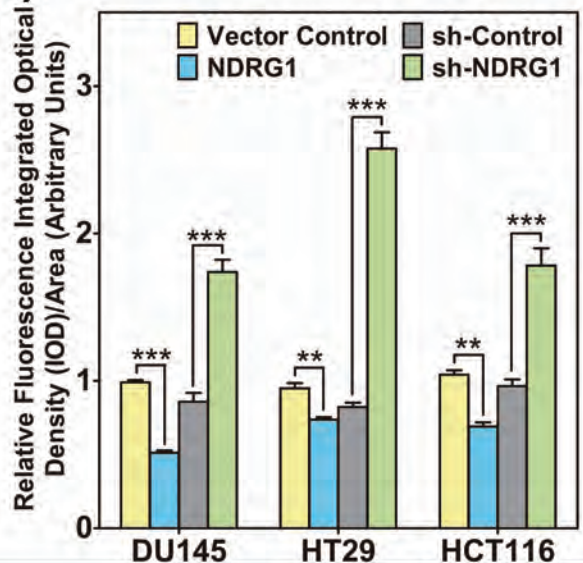
positive control (see lane labeled as "NDRG1"). Densitometric analyses for NDRG1 and ROCK1 are expressed relative to the loading control, β-actin, while that for MLC2 phosphorylation is expressed as the pMLC2/MLC2 ratio. Results are typical of 3-5 experiments and the histograms in (A-C) represent mean ± SD (3-5 experiments). ** $p<0.01$, *** $p<0.001$, relative to the cells treated with Vehicle or Dp2mT.

Figure 9. Iron chelators modulate ROCK1/pMLC2 in prostate and colorectal cancer cells *via* up-regulation of NDRG1. The NDRG1-knockdown clones and their respective sh-Control DU145, HT29 and HCT116 cells were incubated with: Vehicle (0.1% DMSO/medium), Dp2mT (10 μM), DFO (100 μM), Dp44mT (10 μM) or DpC (10 μM) for 24 h. Non-transfected parental cells were included as additional controls to allow comparison between the sh-Control and sh-NDRG1 (see lane labeled as "Control"). Results are typical of 3-5 experiments and the values in histograms in (A-C) represent mean ± SD (3-5 experiments). *** $p<0.001$, relative to cells treated with Vehicle or Dp2mT. ## $p<0.01$, ### $p<0.001$, relative to cells with the same treatment in the sh-Control group.

Figure 10. Schematic illustrating the mechanism of how the metastasis suppressor, NDRG1, affects cellular migration through its ability to inhibit actin filament polymerization, stress fiber assembly and cell migration *via* repressing the ROCK1/pMLC2 pathway in prostate cancer and colorectal cancer cells.
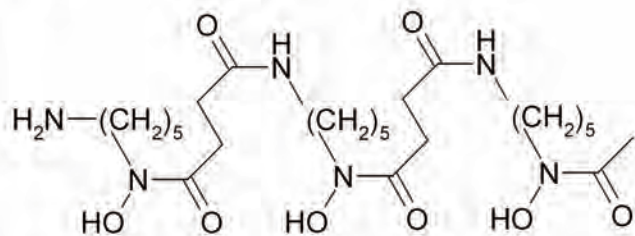
(A) DFO

(B) Dp44mT
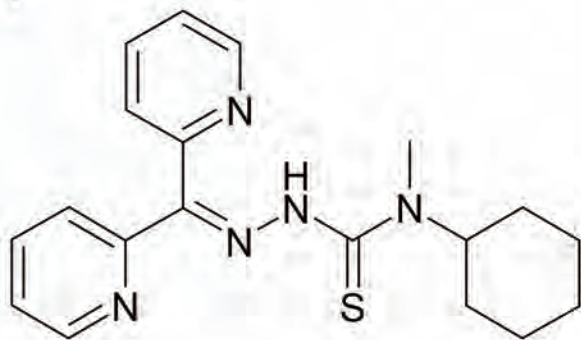
(C) DpC

(D) Dp2mT
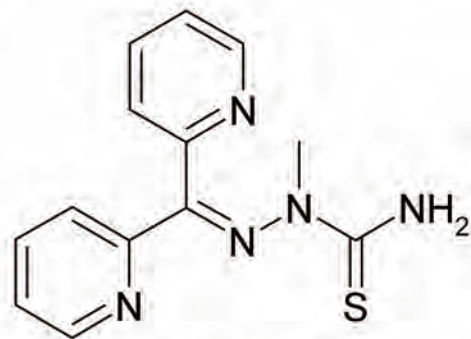
Figure 1

Figure 2

Figure 3

Figure 4

(A) DU145

Vector Control | NDRG1 | sh-Control | sh-NDRG1

Nucleus / F-actin / pMLC2 / Merged

(B) HT29

Vector Control | NDRG1 | sh-Control | sh-NDRG1

Nucleus / F-actin / pMLC2 / Merged

(C) HCT116

Vector Control | NDRG1 | sh-Control | sh-NDRG1

Nucleus / F-actin / pMLC2 / Merged

(D) pMLC2

Vector Control | sh-Control
NDRG1 | sh-NDRG1

Relative Fluorescence Integrated Optical Density (IOD)/Area (Arbitrary Units)
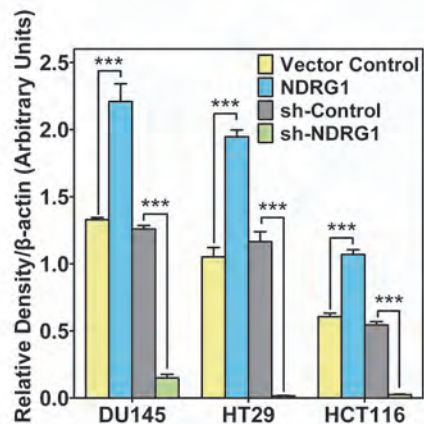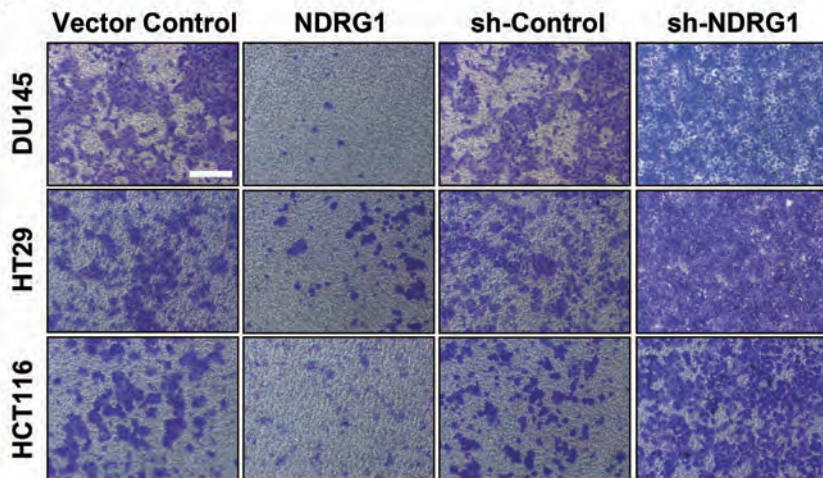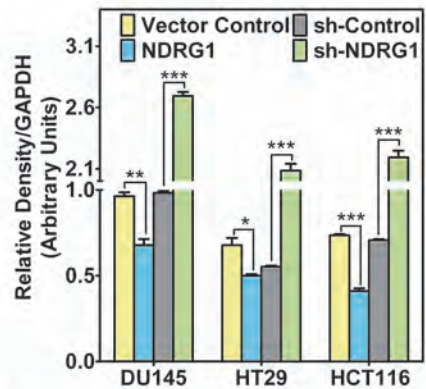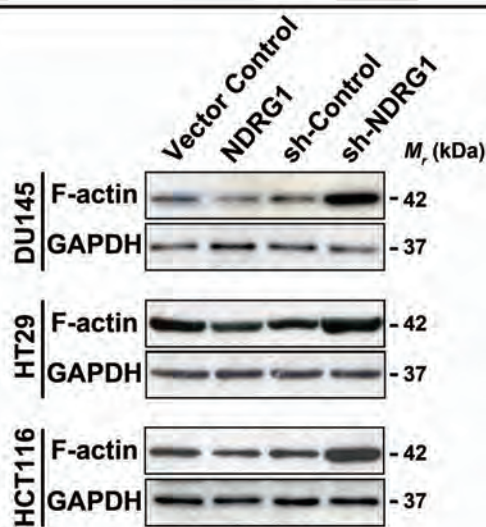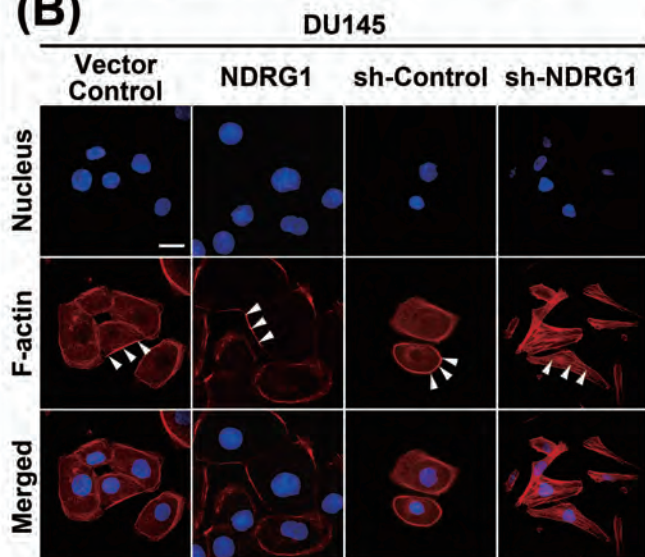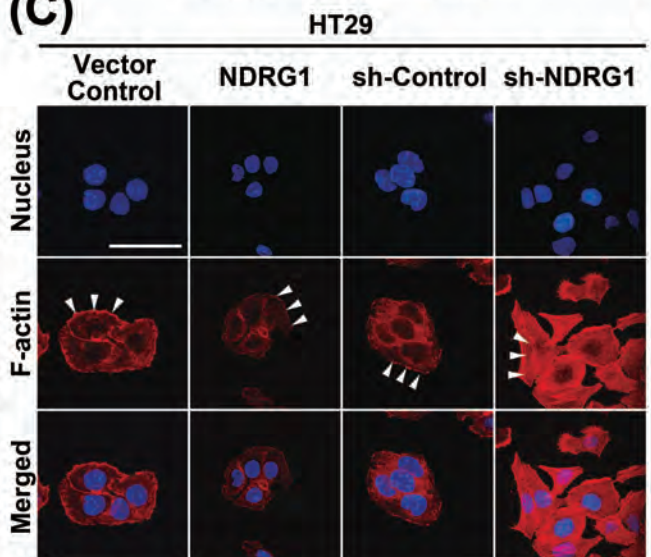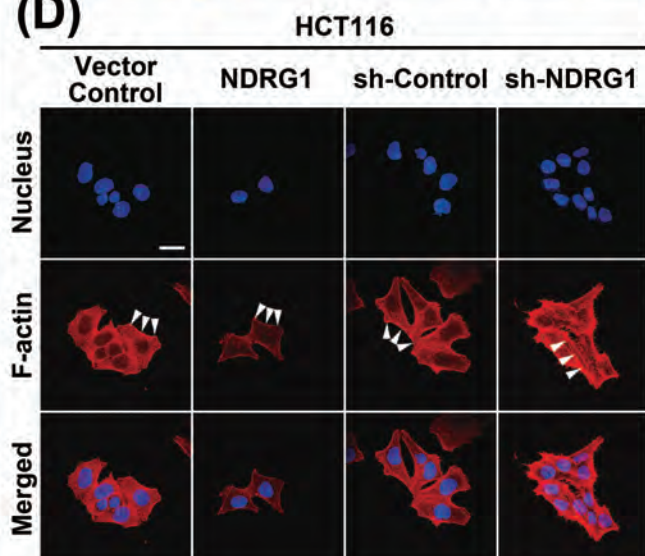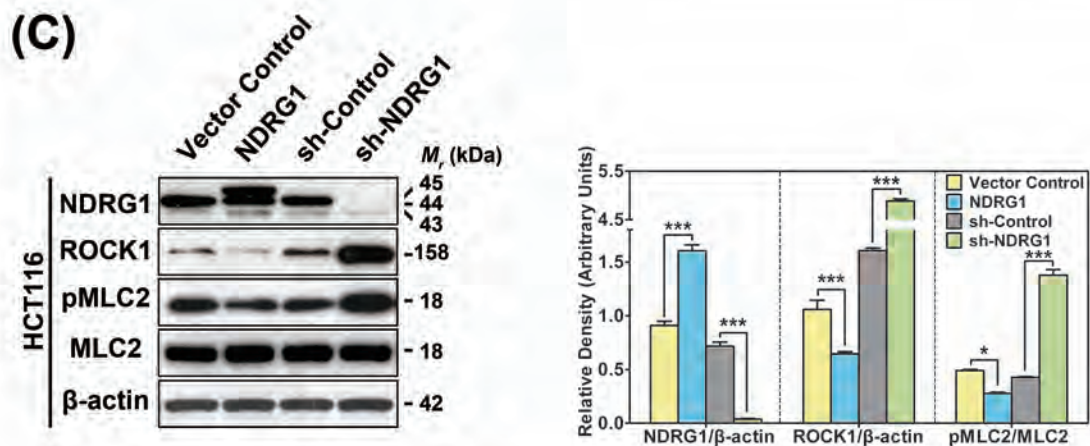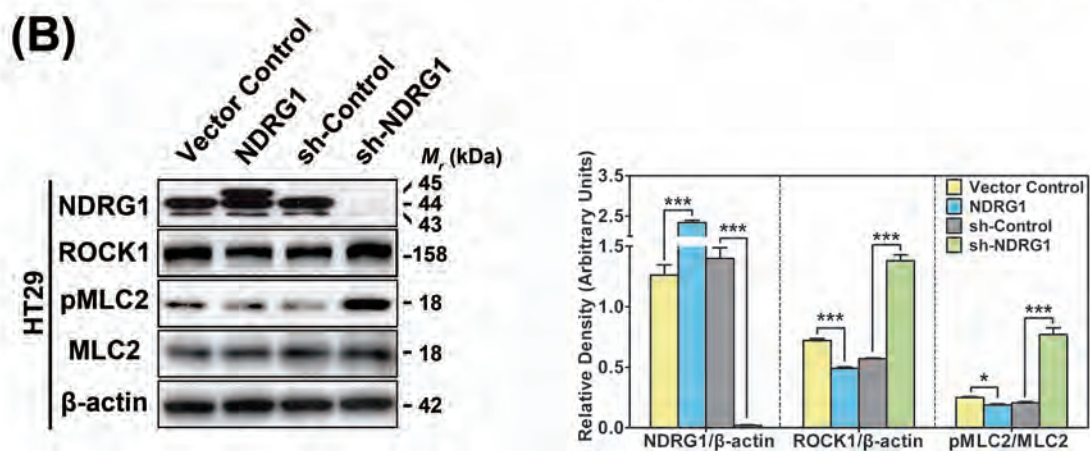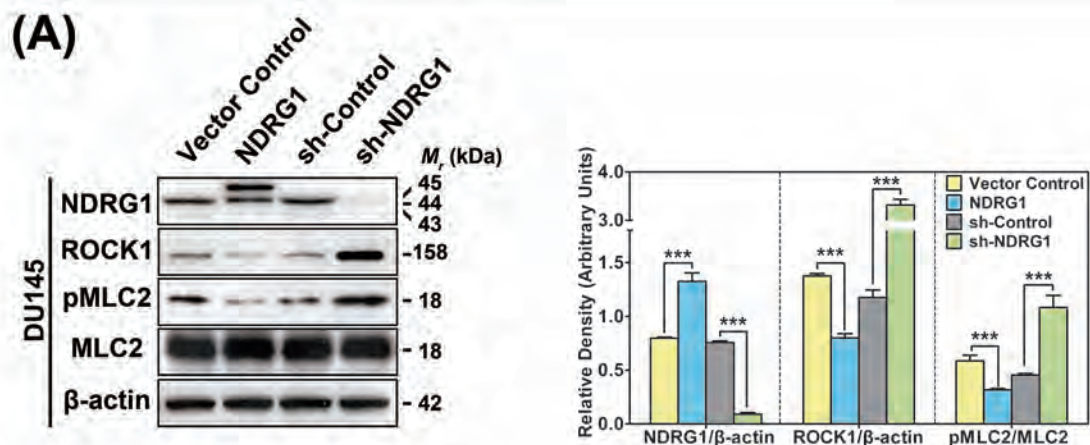
DU145 *** *
HT29 ** ***
HCT116 *** ***
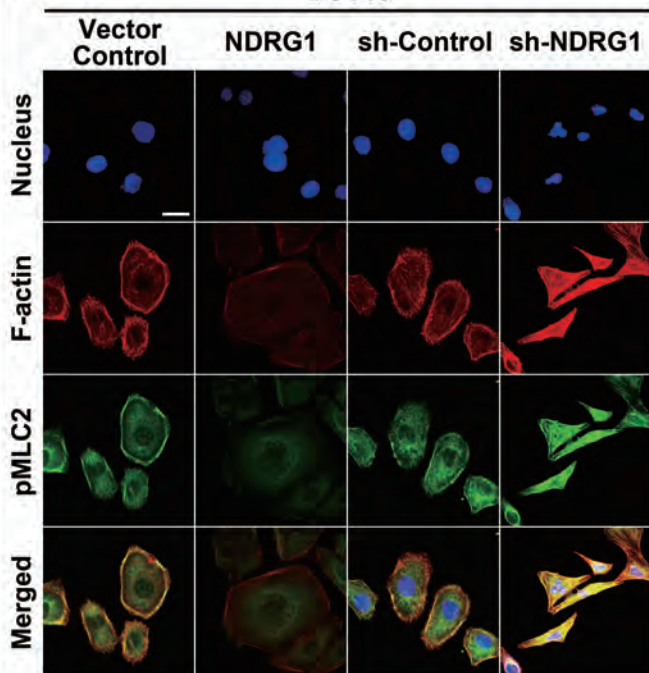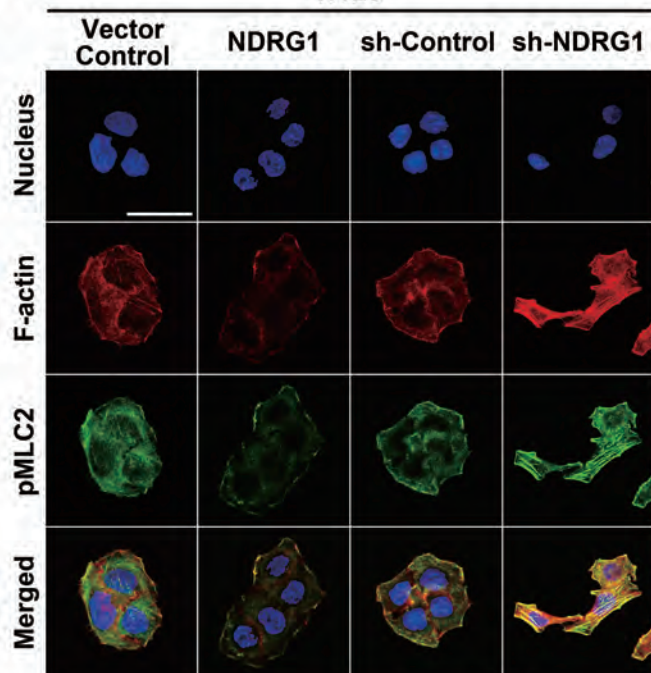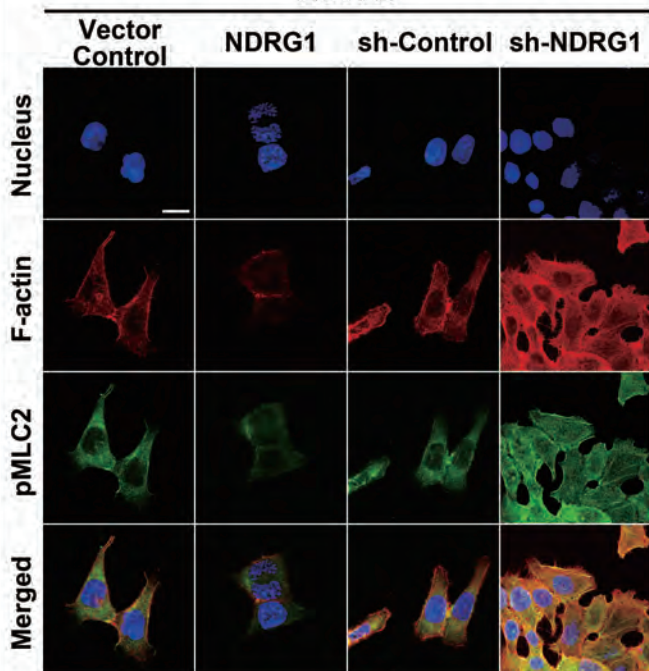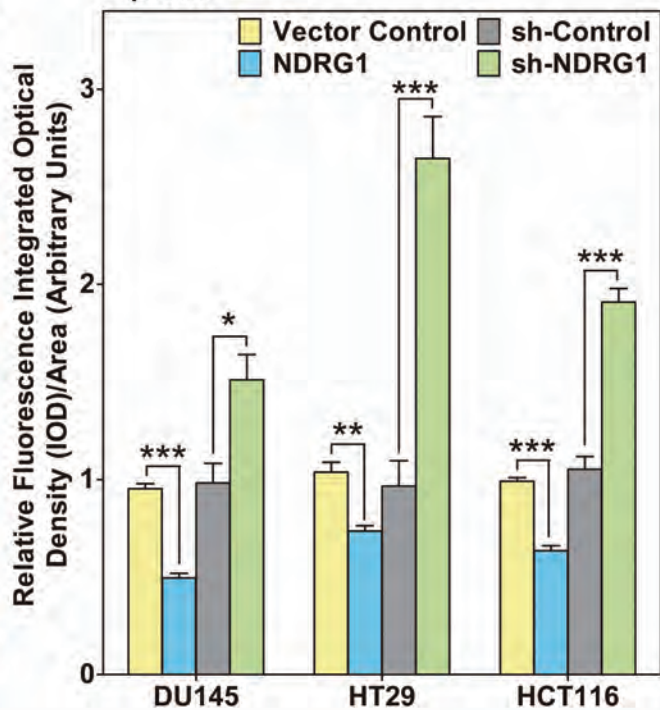
Figure 5

Figure 6

Figure 7

Figure 8

Figure 9

Figure 10